Journal of Subsea and Offshore
-Science and Engineering-, Vol.13

March 30, 2018

Unsteady Yaw Motion Characteristic of A Towed Ship Using Symmetrical Bridle Towline

A. Fitriadhy [a,*], N. Adlina Aldin [b] and N. Aqilah Mansor [b]

[a)] *Programme of Maritime Technology, School of Ocean Engineering, Universiti Malaysia Terengganu, Malaysia*
[b)] *Postgraduate Students, Programme of Maritime Technology, School of Ocean Engineering, Universiti Malaysia Terengganu, Malaysia*

*Corresponding author: a.fitriadhy@umt.edu.my

Paper History

Received: 12-October - 2017
Received in revised form: 6-November-2017
Accepted: 30-March-2108

ABSTRACT

Instability of a ship towing system indicated by vigorous yaw motion of a towed ship may reduce the safety of the navigation especially in the restricted with heavy congestion waterways. To stabilise this towing system, a comprehensive investigation on a towline configuration is therefore required. This paper presents Computational Fluid Dynamic (CFD) approach to analyse the unsteady yaw motion characteristic of a towed ship using symmetrical bridle towline. Several towing parameters such as various towing point locations on the symmetrical bridle towline and towing's velocity have been taken into account. Here, a towed ship designates as 1B (barge) is employed in the simulations. The results revealed that the subsequent increase of towing point location on the symmetrical bridle towline will reduce significantly her unsteady yaw motions by 99.67%, improves barge course stability. In addition to increasing towing's velocity, it gradually leads to have poor course stability as the yaw motion increased by 23.83% meanwhile slewing period decreased by 20% as velocity increased.

KEY WORDS: *Yaw Motion, CFD, Towing Point, Towline Length, And Course Stability.*

NOMENCLATURE

CFD	Computational Fluid Dynamic
1B	Barge
l'	Ratio of towline length with respect to length of barge
l'_b	Ratio of tow point location with respect to barge length
V_s	Tug's velocity
RANSE	Reynolds-Averaged Navier Stokes Equation

1.0 INTRODUCTION

The drastic growth of shipping activities leads to heavy congestion due to abundant of ships in the waterways that threaten the safety navigation of a towed ship. If the towing stability of a towed vessel is not secure, it can cause monetary losses due to delayed arrival and marine accidents due to large irregular behavior [14]. Therefore, an extensive course stability investigation is then required to observe towed barge using symmetrical bridle towline behavior during the operations.

In recent years, several studies regarding course stability of a ship towing system investigating motion characteristics of the towed ship. Several researchers have presented numerous investigations in typical towline configuration; single towline model. [1, 2, 8, 9] performed a theoretical approach in investigating towing system by using an elastic towline. [3] investigates the problem by using steel wire rope while [11] studied the dynamics of coupled tug-towed system connected by means of a rigid towline. [4], [5] performed numerical approach by treated the towline as non-extensible catenary model using lumped mass approach, then, extended the research by introducing a symmetrical bridle towline configuration compared to traditional ways; single towline model. [7, 15] presented experimental approach of towing system, however, [14, 15] introduced new towline configuration, a symmetrical towline configuration. A towing bridle can be used to improve the towing stability of a towed vessel [14]. A reliable simulation is then required to stabilize the system compared to theoretical approach which impractical, more time and cost consuming.

JSOse | Received: 12-Octobere-2017 | Accepted: 30-March-2018 | [(13) 1: 1-7]
Published by International Society of Ocean, Mechanical and Aerospace Scientists and Engineers, www.isomase.org., ISSN: 2442-6415

Thus, this paper presents a CFD simulation to predict the effects of symmetrical bridle towline model to course stability of towed barge (1B). Here, a commercial CFD so called Flow3D v10.1 is utilized by applying unsteady Reynolds-Averaged Navier Stokes Equation (RANSE).

2.0 GOVERNING EQUATION

The CFD flow solver on FLOW-3D version 10.1 is based on the incompressible unsteady RANS equations in which the solver applies the Volume of Fluid (VOF) to track the free surface elevation. The interface between fluid and solid boundaries is simulated with the fractional area volume obstacle representation favour method. This method computes open area and volume in each cell to define the area that is occupied by obstacle.

2.1 Continuity and Momentum Equation

The continuity and momentum equations for a moving object and the relative transport equation for VOF function are

$$\frac{V_f}{\rho}\frac{\partial \rho}{\partial t}+\frac{1}{\rho}\nabla\cdot\left(\rho\vec{u}A_f\right)=-\frac{\partial V_f}{\partial t} \quad (1)$$

$$\frac{\partial \vec{u}}{\partial t}+\frac{1}{V_f}\left(\vec{u}A_f\cdot\nabla\vec{u}\right)=-\frac{1}{\rho}\left[\nabla_\rho+\nabla\cdot\left(\tau A_f\right)\right]+\vec{G} \quad (2)$$

$$\frac{\partial F}{\partial t}+\frac{1}{V_f}\nabla.\left(F\vec{u}A_f\right)=-\frac{F}{V_f}\frac{\partial V_f}{\partial t} \quad (3)$$

where ρ is the density of the fluid, $\vec{u}$ is the fluid velocity, V_f is the volume fraction, A_f is the area fraction, p is the pressure, τ is the viscous stress tensor, G denotes gravity and F is the fluid fraction.

In the case of coupled GMO's motion, Eqs.(1) and (2) are solved at each time step and the location of all moving objects is recorded and the area and volume fractions updated using the FAVOR technique. Equations (3) are solved with the source term $\left(-\frac{\partial V_f}{\partial t}\right)$ on the right-hand side which is computed as

$$-\frac{\partial V_f}{\partial t}=\vec{U}_{obj}.\vec{n}S_{obj}/V_{cell} \quad (4)$$

where S_{obj} is the surface area, $\vec{n}$surface normal vector, $\vec{U}_{obj}$ is the velocity of the moving object at a mesh cell and V_{cell} is the total volume of the cell [6]

2.2 Turbulence model

The transport equation for k_T includes the convection and diffusion of the turbulent kinetic energy, the production of turbulent kinetic energy due to shearing and buoyancy effects, diffusion, and dissipation due to viscous losses within the turbulent eddies. Buoyancy production only occurs if there is a non-uniform density in the flow, and includes the effects of gravity and non-inertial accelerations. The transport equation is:

$$\frac{\partial k_T}{\partial t}+\frac{1}{V_F}\left\{uA_x\frac{\partial k_T}{\partial x}+vA_y\frac{\partial k_T}{\partial y}+wA_z\frac{\partial k_T}{\partial z}\right\}=P_T+G_T+Diff_{k_T}-\varepsilon_T \quad (5)$$

Where V_F, A_x, A_y *and* A_z are FLOW-3D's FAVOR™ functions, P_T is the turbulent kinetic energy production:

$$P_T=CSPRO\left(\frac{\mu}{pV_F}\right)\times\left\{\begin{array}{c}2A_x\left(\frac{\partial \mu}{\partial x}\right)^2+2A_y\left(R\frac{\partial v}{\partial y}\xi\frac{u}{x}\right)^2+2A_z\left(\frac{\partial w}{\partial z}\right)^2\\+\left(\frac{\partial v}{\partial x}+R\frac{\partial \mu}{\partial y}+\xi\frac{v}{x}\right)\left[A_x\frac{\partial v}{\partial x}+A_y\left(R\frac{\partial u}{\partial y}+\xi\frac{v}{x}\right)\right]\\+\left(\frac{\partial u}{\partial z}+\frac{\partial w}{\partial x}\right)\left(A_z\frac{\partial u}{\partial z}+A_x\left(R\frac{\partial w}{\partial x}\right)\right)\\+\left(\frac{\partial v}{\partial z}+R\frac{\partial w}{\partial y}\right)\left(A_z\frac{\partial v}{\partial z}+A_yR\frac{\partial w}{\partial y}\right)\end{array}\right\} \quad (6)$$

where CSPRO is a turbulence parameter.

In the case of this computation for turbulent condition, $k-\varepsilon$ model is proposed where k_T and ε_T are the turbulent kinetic energy and turbulent dissipation energy, respectively. Two transport equations for the turbulent kinetic energy k_T and its dissipation ε_T so-called $k-\varepsilon$ model are used in the computational simulation. It is reasonable since this equation model provides more reliable approximations to many types of flows [6]. In addition, $k-\varepsilon$ model is quite economical in terms of CPU time, compared to, for example the SST turbulence model, which increases the required CPU times by nearly 25%. [10] stated $k-\varepsilon$ model reduced the computational time and resources by reducing the number of nodes in the near wall regions, which allow for more probing simulation and trial geometries.

2.3 Body motion computation

The body motion is analysed in a space-fixed Cartesian coordinate system, the global coordinate system. The governing equation of the six degree of freedom (DOF) of a rigid body motion can be expressed in this coordinate system as

$$\frac{d}{dt}(m\vec{v}_C)=\vec{f} \quad (7)$$

$$\frac{d}{dt}(M_C.\vec{\omega}_C)=\vec{m}_C \quad (8)$$

The index C denotes the centre of mass of the body, m denotes the mass of the body, $\vec{v}_c$the velocity vector, M_c is the tensor of the moments of inertia, $\vec{\omega}_c$is the angular velocity vector, $\vec{f}$ denotes the resulting force vector and $\vec{m}_c$ denotes the resultant moment vector acting on the body [12]. The resultant force $\vec{f}$ has three components; surface force, field forces and external forces:

$$\vec{f}=\int_S(T-\rho I).\vec{n}dS+\int_V\rho_b\vec{b}dV+\vec{f}E \quad (9)$$

Here, ρ_b is the density of the body. The only field force considered is the gravity, so the volume integral of above equation (right hand side) reduces to $m\vec{g}$, where g is the gravity acceleration vector. The vector $f\vec{E}$ denotes the external forces acting in the body [13].

JSOse | Received: 12-Octobere-2017 | Accepted: 30-March-2018 | [(13) 1: 1-7]
Published by International Society of Ocean, Mechanical and Aerospace Scientists and Engineers, www.isomase.org., ISSN: 2442-6415

3.0 SIMULATION CONDITIONS

3.1 Principal Data of Ship

The principal dimensions barge (1B) are presented in Table 1. Her respective body plan is shown in Figure 1.

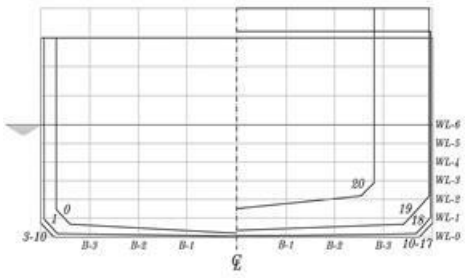

Figure 1: Body plan of barge (right).

Table 1: Principal dimensions of barge (1B).

	1B	
Description	Full-scale	Model
Length, *L(m)*	60.96	1.219
Breadth, *B(m)*	10.67	0.213
Draft, *d(m)*	2.74	0.0548
Volume, $V(m^3)$	1646.2	0.01317
L/B	5.71	5.71
Block coefficient,C_b	0.92	0.92
k_{yy2}/L	0.3266	0.3266
$X_{G\ abaft\ the\ midship}$,$(m)$	-1.04	-0.0208

3.2 Parametric Studies

Table 2 shows various of tow point location, l_b' used in the simulation. Towing's velocity are kept constant of 0.509 m/s.

The tug is replaced with the sphere by using similar characteristics of a tug. Various towing's velocity, V_s is shown in Table 3 while towpoint location is set to l_b'=0.75.

Table 2: Various tow point location.

Towing's velocity, V_s (m/s)	Tow point, l_b'
0.509	0.5
	0.75
	1.0

Table 3: Various towing's velocity

Towing's velocity, V_s (m/s)	Tow point, l_b'
0.509	
0.582	
0.6549	0.75
0.7276	

3.3 Computational Domain and Boundary Conditions

The computational domain uses a structured mesh that is defined in a Cartesian. Referring to Figure 2, the boundary condition is mark in the mesh block. The boundary condition at X-max boundary is specified velocity so that there is flow of water. In order to save computational time, velocity of 0.509 m/s is given to water at X-max boundary. As for X-min, Y-max and Y-min boundary, outflow is assigned to prevent reflection while Z-min is specified pressure and Z-max is symmetry. The boundary conditions for this simulation are shown in Table 4.

Table 4: Boundary condition

Boundary	Conditions
X_{min}	Specified velocity
X_{max}	Outflow
Y_{min}	Outflow
Y_{max}	Outflow
Z_{min}	Symmetry
Z_{max}	Specified pressure

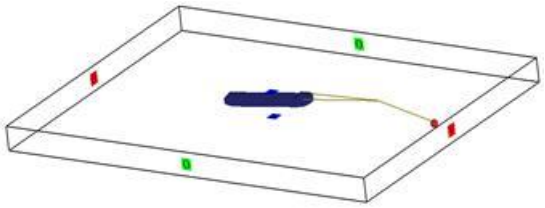

Figure 2: Boundary conditions

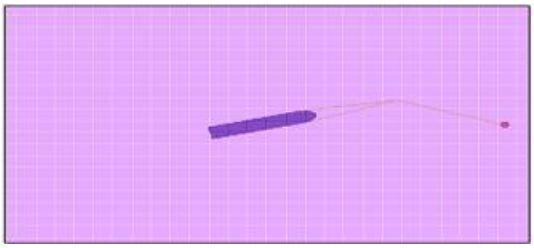

Figure 3: Meshing generation

The barge is coupled through a towline. Sphere model which acted as the tow ship is assigned prescribed motion while barge as towed ship was set as coupled motion in X-translational, Y-translational and Z-rotational motions (surge, sway and yaw motions). The barge was in 15° inclination arrangement initially. The towline is set as massless elastic rope with spring coefficient of 2 N/m^2.

Based on the applications of Flow3D v10.1.1, the average duration of every simulation was about 70-80 hours (4 parallel computations) on a HP Z820 workstation PC with processor Intel (R) Xeon (R) CPU ES-2690 v2 @ 3.00 GHz (2 processors) associated with the installed memory (RAM) of 32.0 GB and 64-bit Operating System.

4.0 RESULT AND DISCUSSIONS

Figures 4 - 7 show the CFD simulations have been successfully carried out to predict the course stability of the towing system in the various towline length and towing velocity. The simulations results of sway and yaw motions of the barge associated with the towline tension are discussed.

JSOse | Received: 12-Octobere-2017 | Accepted: 30-March-2018 | [(13) 1: 1-7]
Published by International Society of Ocean, Mechanical and Aerospace Scientists and Engineers, www.isomase.org., ISSN: 2442-6415

4.1 Effect of Tow point Location

The characteristics of sway and yaw motion in various tow point location is displayed in Figure 4. Increasing tow point location from l_b'= 0.5 to 0.75 and 1.0 resulted in significant decrement of yaw motion by 26.9 % and 99.54% respectively. The fishtailing period of 1B was lowered by 9.09% as tow point location increased from l_b'= 0.5 to 1.0. It was noted that sway motion decreased by 69.94% as the tow point location is increased from l_b'= 0.5 to 1.0. The course stability of 1B was improve as as increasing tow point location decreased sway motion of barge. As remarked in the numerical approach by [4], the slewing motion was decrease as the tow point was increased from l_b'= 0.5 to 0.75. The towline tension showed insignificant decrement, however, further increase of l_b' would diminish the unwieldy slewing motion, which leads to better towing stability. Based on Figure 5 which shows free surface elevation, it can be explained that l_b' = 0.5 shows vigorous sway motion compare to l_b'= 0.75 and l_b'= 1.0.

4.2 Effect of Towing's velocity

Figure 6 shows the characteristics of sway and yaw motion associated with dynamic towline tension in various towing velocity. The subsequent increase of towing velocity from Vs= 0.509 to 0.6549 m/s resulted in increment of sway motion by 3.98%. However, the lateral motion of the barge decreasing by 2.85% due to increasing towing velocity from 0.6549 to 0.7276 m/s. The yaw motion of the barge increased by 23.83% as the tug's speeding from V_s= 0.509 to 0.7276 m/s. Reduction of slewing period by 20% resulted due to increasing towing's velocity. Higher wave crest (dark colour) present at the bow region and prone to increase as the velocity increased from V_s= 0.509 to 0.7276 m/s which proportional to high pressure (see Figure 7).

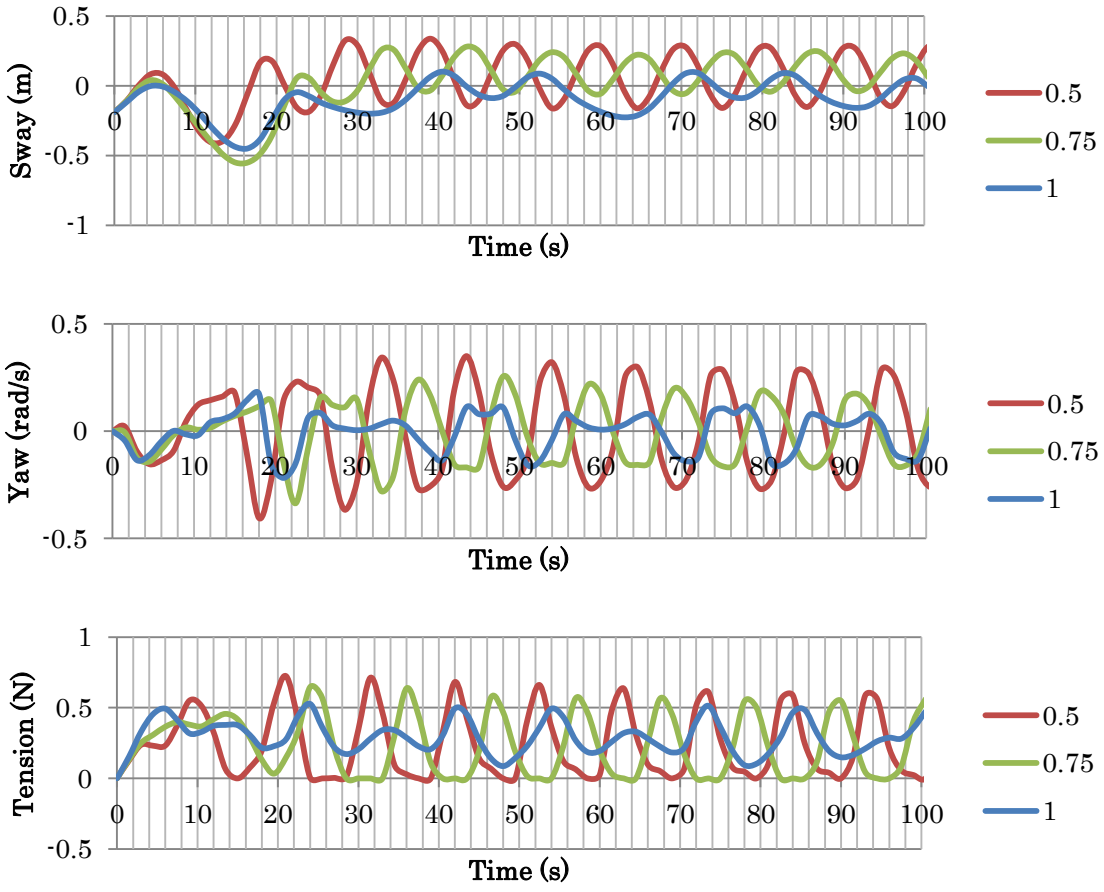

Figure 4: Characteristics of sway and yaw motion of 1B associated with the towline tension at various towpoint location

JSOse | Received: 12-Octobere-2017 | Accepted: 30-March-2018 | [(13) 1: 1-7]
Published by International Society of Ocean, Mechanical and Aerospace Scientists and Engineers, www.isomase.org., ISSN: 2442-6415

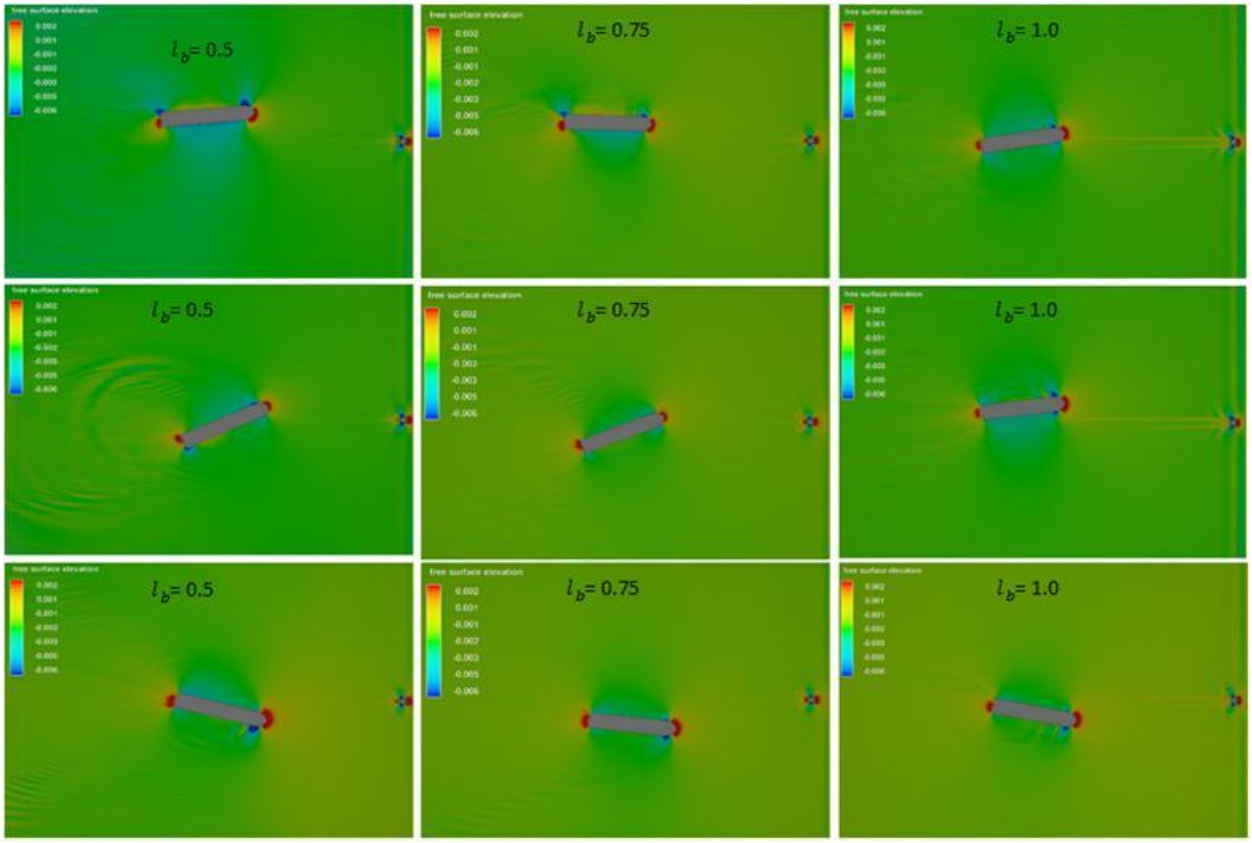

Figure 5: Free surface elevation, Vs= 0.509, l_b' = 0.5(left), 0.75 (middle), and 1.0 (right)

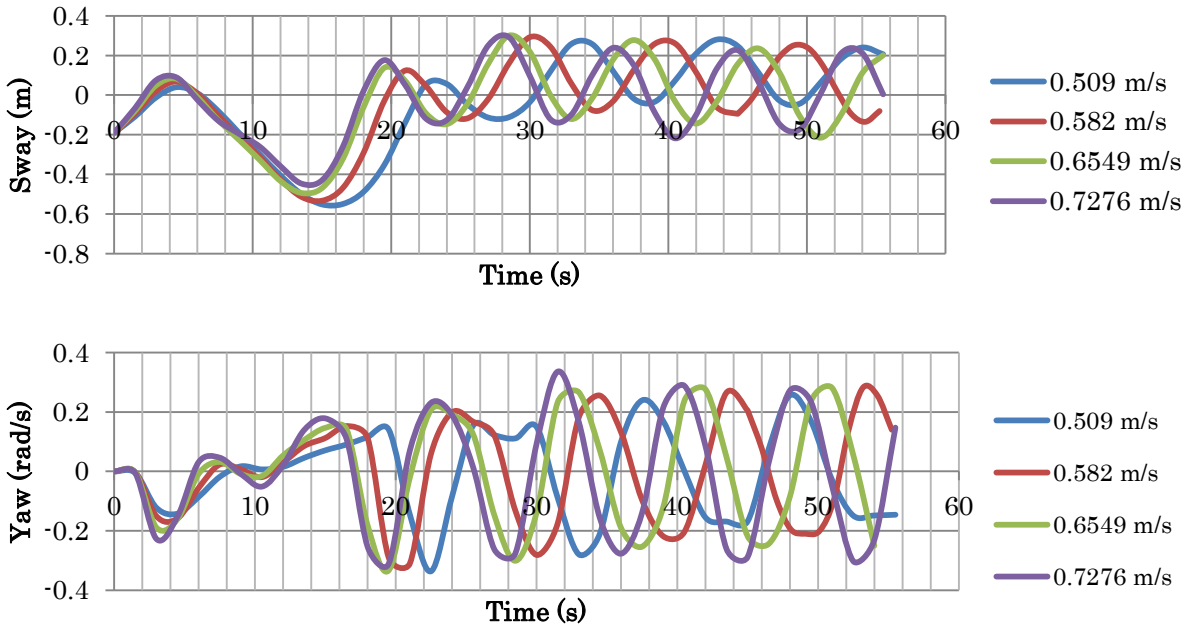

JSOse | Received: 12-Octobere-2017 | Accepted: 30-March-2018 | [(13) 1: 1-7]
Published by International Society of Ocean, Mechanical and Aerospace Scientists and Engineers, www.isomase.org., ISSN: 2442-6415

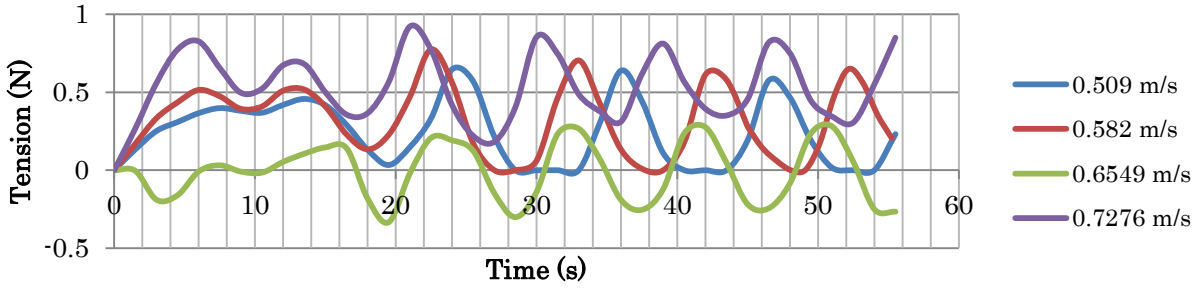

Figure 6: Characteristics of sway and yaw motion of 1B associated with the towline tension at various towing's velocity

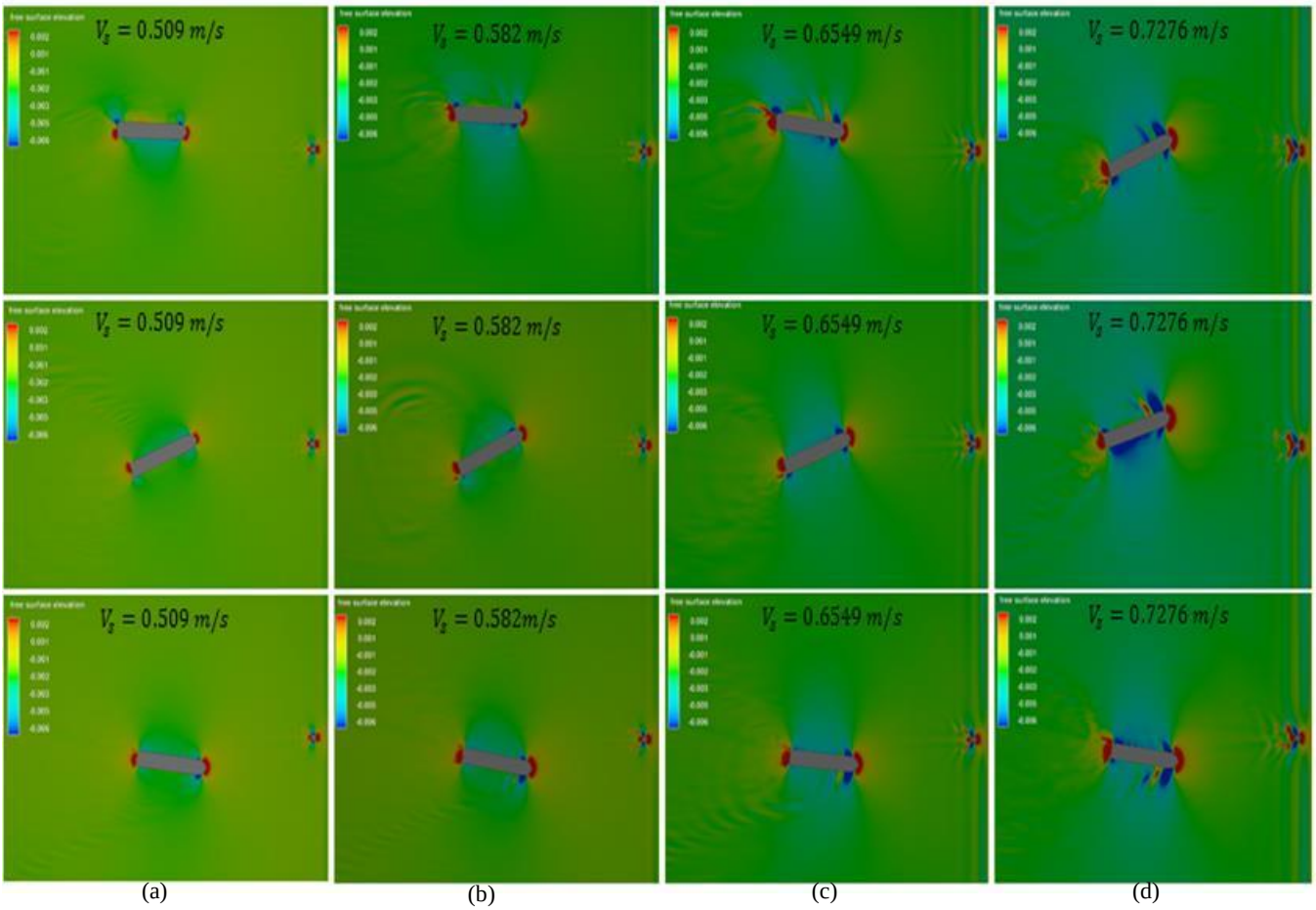

(a) (b) (c) (d)

Figure 7: Free surface elevation, l_b' = 0.75, Vs= (a) 0.509, (b) 0.582, (c) 0.6549 and (d) 0.7276 m/s

5.0 CONCLUSION

The Computational Fluid Dynamics (CFD) analysis on the course stability of the ship's towing system was successfully performed using FLOW3D version 10.1 software. The effects of different towline length and towing's velocity were investigated. The simulation results are as follows:

- Extending tow point location (l_b') from 0.5 to 1.0 was improving course stability of the barge indicated by decrement of sway and yaw motion. However, the slewing period decreasing by 9.09% and 10% from l_b'= 0.5 to l_b'=0.75 and l_b'=1.0, respectively, while the towline tension decreases by 27.2%.
- The increase of towing's velocity from V_s =0.509 m/s to 0.6549 m/s increased the sway motion by 6.71%, while yaw motion slightly decreased from V_s= 0.582 to 0.7276 m/s by 23.83%. Meanwhile towline tension increased by 29.83% from V_s=0.509 to 0.7276 m/s.

JSOse | Received: 12-Octobere-2017 | Accepted: 30-March-2018 | [(13) 1: 1-7]
Published by International Society of Ocean, Mechanical and Aerospace Scientists and Engineers, www.isomase.org., ISSN: 2442-6415

ACKNOWLEDGEMENTS

The authors greatly appreciate to Ministry Higher Education of Malaysia for the financial support awarded from Fundamental Research Grant Scheme (FRGS) VOT NO 59414.

REFERENCE

1. Bernitsas, M. and Kekridis, N. (1985). *Simulation and Stability of Ship Towing*. International Shipbuilding Progress, 32(369), 112-123.
2. Bernitsas, M.M. and Chung, J.-S. (1990). *Nonlinear Stability and Simulation of Two-line Ship Towing and Mooring*. Applied Ocean Research, 12(2), 77-92.
3. Fang, M.-C. and Ju, J.-H. (2009). *The Dynamic Simulations of the Ship Towing System in Random Waves*. Marine Technology, 46(2), 107-115.
4. Fitriadhy, A. and Yasukawa, H. (2011). *Course Stability of a Ship Towing System*. Ship Technology Research, 58(1), 4-23.
5. Fitriadhy, A., Yasukawa, H. and Koh, K. (2013). *Course Stability of a Ship Towing System in Wind*. Ocean Engineering, 64, 135-145.
6. *Flow3D 10.1.1 User Manual*. (2013). Flow Science Inc.
7. Kume, K., Hasegawa, J., Tsukada, Y., Fujisawa, J., Fukasawa, R. and Hinatsu, M. (2006). *Measurements of Hydrodynamic Forces, Surface Pressure, and Wake for Obliquely Towed Tanker Model and Uncertainty Analysis for CFD Validation*. Journal of marine science and technology, 11(2), 65-75.
8. Lee, M.-L. (1989). *Dynamic Stability of Nonlinear Barge-towing System*. Applied mathematical modelling, 13(12), 693-701.
9. Sinibaldi, M. and Bulian, G. (2014). *Towing Simulation in Wind through a Nonlinear 4-DOF Model: Bifurcation Analysis and Occurrence of Fishtailing*. Ocean Engineering, 88, 366-392.
10. Talaat, W.M., Hafez, K. and Banawan, A. (2017). *A CFD Presentation and Visualization For a New Model that Uses Interceptors to Harness Hydro-energy at the Wash of Fast Boats*. Ocean Engineering, 130, 542-556.
11. Varyani, K.S., Barltrop, N.D. and Pham, X.P. *Fishtailing Instabilities in Emergency Towing of Disabled Tankers*. in *The Fifteenth International Offshore and Polar Engineering Conference*. 2005. International Society of Offshore and Polar Engineers.
12. Wu, C.-S., Zhou, D.-C., Gao, L. and Miao, Q.-M. (2011). *CFD Computation of Ship Motions and Added Resistance for a High Speed Trimaran in Regular Head Waves*. International Journal of Naval Architecture and Ocean Engineering, 3(1), 105-110.
13. Yan, S. and Huang, G. (1996). *Dynamic Performance of Towing System-Simulation and Model Experiment*. Proceedings, OCEAN, 96.
14. You, Y.J., Hur, J. and Jung, J. (2015). *An Experimental Study on an Auxiliary Towing System for an FPSO using Active Thrusters*. Applied Ocean Research, 52, 62-72.
15. Zan, U.I., Yasukawa, H., Koh, K.K. and Fitriadhy, A. (2012). *Model Experimental Study of a Towed Ship's Motion*. The 6th Asia-Pacific Workshop on Marine Hydrodymics-APHydro.

JSOse | Received: 12-Octobere-2017 | Accepted: 30-March-2018 | [(13) 1: 1-7]
Published by International Society of Ocean, Mechanical and Aerospace Scientists and Engineers, www.isomase.org., ISSN: 2442-6415